Structure of Iron Ions in Some Acetone Based Electrolytes

ARTICLE *in* THE JOURNAL OF PHYSICAL CHEMISTRY A · MARCH 2013

Impact Factor: 2.69 · DOI: 10.1021/jp400556d · Source: PubMed

4 AUTHORS, INCLUDING:

Wojciech Olszewski
Cells Alba
30 PUBLICATIONS **76** CITATIONS
SEE PROFILE

Dariusz Satula
University of Bialystok
88 PUBLICATIONS **433** CITATIONS
SEE PROFILE

Beata Kalska-Szostko
University of Bialystok
42 PUBLICATIONS **173** CITATIONS
SEE PROFILE

THE JOURNAL OF PHYSICAL CHEMISTRY A

Article

pubs.acs.org/JPCA

Structure of Iron Ions in Some Acetone Based Electrolytes

Wojciech Olszewski,*[,†] Krzysztof Szymański,[†] Dariusz Satuła,[†] and Beata Kalska-Szostko[‡]

[†]Faculty of Physics, University of Bialystok, ul. Lipowa 41, 15-424 Białystok, Poland

[‡]Institute of Chemistry, University of Bialystok, ul. Hurtowa 1, 15-399 Białystok, Poland

ABSTRACT: X-ray absorption, Mössbauer, and Raman spectroscopy were combined to determine the local environment of iron ions in acetone based solutions of $FeCl_2$. It is shown that part of the Fe(II) ions change their oxidation state, accompanied by symmetry change from octahedral $Fe(H_2O)_6^{2+}$ to tetrahedral $[FeCl_4]^-$ at large acetone concentrations. The ratio of Fe(II)/Fe(III) determined by Mössbauer spectroscopy agrees well with that determined by the X-ray absorption studies. Raman measurements confirm quantitative estimations of $[FeCl_4]^-$ species in acetone rich solutions.

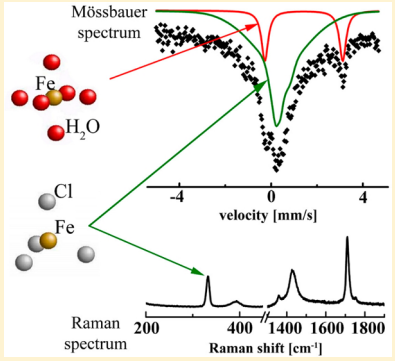

1. INTRODUCTION

Metal ions have a strong tendency to form complexes with oxygen donor ligands. Numerous studies of the structure and bonding of aqua complexes have shown that the majority of small and medium sized di- and trivalent cations form hexaaqua complexes in aqueous solutions.[1−3]

Recently, the new acetone based electrolyte for metal layer electroplating was developed.[4,5] Extended X-ray absorption fine structure (EXAFS) analysis combined with ab initio X-ray absorption near edge (XANES) structure calculations was successfully applied to solve the local structure of iron ions in water and acetone solutions at a certain concentration range. In the case of solutions rich in acetone, the experimental data were reproduced assuming that the majority of iron ions form complexes with tetrahedral Cl^- arrangement and the rest octahedral $Fe(H_2O)_6^{2+}$.[6] The obtained values of the structural parameters were in good agreement with previously reported values for those complexes.[1,7−9] The samples for experiments[6] were prepared from $FeCl_2$ with sufficient care to avoid oxidation of Fe(II) by oxygen, either atmospheric or dissolved in the solvents, and the results of X-ray analysis were explained consistently assuming the presence of Fe(II) ions only. We have observed that acetone rich solutions prepared from $FeCl_2$ have dark brown color, characteristic of Fe(III). As it was shown by Garcia et al.[1] and Benfatto et al.,[10] the change of oxidation state of iron from Fe(II) to Fe(III) leads to a shift of the absorption edge by 4.5−5 eV, not detected in our experiment.[6]

Mössbauer spectroscopy can resolve unambiguously the problem of the oxidation state of iron in acetone rich solutions, while Raman spectroscopy is sensitive to changes in molecular symmetry. The goal of this paper is to characterize the local structure of diluted iron ions in some part of the ternary $C_3H_6O-H_2O-HCl$ phase diagram of system, interesting for potential applications, by combined methods, X-ray absorption spectroscopy (XAS), Mössbauer, and Raman spectroscopy.

2. EXPERIMENTAL SECTION

2.1. Materials. The samples were prepared using $FeCl_2 \cdot 4H_2O$ dissolved in solutions composed of acetone, water, and hydrogen chloride in two series. In the first series, the amount of hydrogen chloride (0.2 wt %) was constant and the concentration of water was varied in the 4.7−99.6 wt % range. In the second series, the hydrogen chloride concentration was varied in the 0.0−0.2 wt % range. Reagents were deoxygenated and mixed under argon atmosphere to avoid accidental oxidation of Fe(II) to Fe(III) ions. Some reference samples were prepared using $FeCl_3 \cdot 6H_2O$. All samples contained 0.2 wt % iron.

2.2. Methods. Details of XAS measurements performed on the K-edge of iron in some solutions were presented in Olszewski et al.[6]

^{57}Fe Mössbauer spectra of the frozen solutions were recorded with a conventional Mössbauer spectrometer in transmission geometry at 40 K in a closed cycle He cryostat. A ^{57}Co(Cr) source was used, and the spectrometer was calibrated with 6 μm α-Fe foil at room temperature, which is the reference for isomer shift reported in this paper. The Mössbauer spectra were analyzed by least-squares fitting of the Lorentzian lines with the help of the NORMOS program.[11]

Raman spectra of solutions were acquired under ambient conditions using a Renishaw Raman spectrometer equipped with a 514 nm wavelength argon laser source and high sensitivity ultralow noise CCD detector. The laser power was set at 5−25 mW in order to avoid laser-induced decomposition

Received: January 17, 2013
Revised: February 20, 2013
Published: February 20, 2013

   dx.doi.org/10.1021/jp400556d | J. Phys. Chem. A 2013, 117, 2190−2194

of the samples. All solutions were stored in 1 cm diameter glass vials.

3. RESULTS AND DISCUSSION

3.1. XAS Spectra. The details of the analysis of representative XAS spectra and determination of octahedral and tetrahedral local structures of iron ion in some C_3H_6O−H_2O−HCl solutions were already presented.[6] XAS spectra in a much more complete concentration range are presented in Figure 1. By decreasing the H_2O concentration, one observes

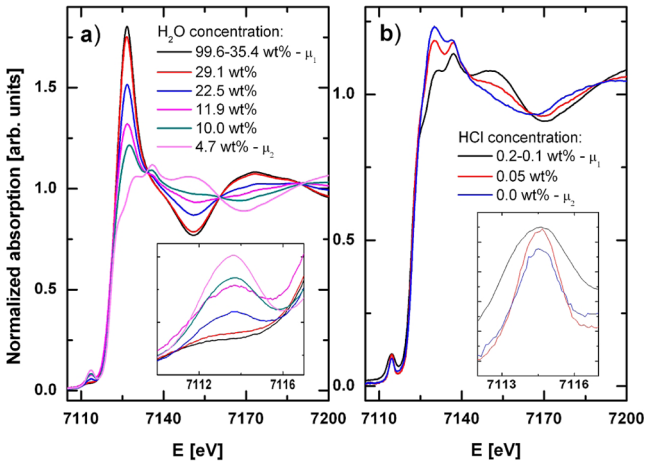

Figure 1. XAS spectra as a function of (a) H_2O and (b) HCl concentrations. The insets correspond to the pre-edge region for the same concentrations as in the main graph. Spectra of samples in the concentration range 35.4−99.6 H_2O wt % and 0.1−0.2 HCl wt % have the same shape, shown by a single black line. Solutions at extreme compositions are abbreviated by μ_1 and μ_2 in the legend.

an increase in the intensity of the pre-edge peak at 7113 eV (associated with the 1s−3d transition) and a decrease in the white line intensity at 7126 eV (1s−4p transition). The decrease in the HCl concentration results in the opposite effect: the decrease in the pre-edge peak's intensity and the increase in the white line intensity.

Those features can be unambiguously related to the changes in the iron ion's first coordination shell, from octahedral to tetrahedral symmetry, upon the decrease in water (Figure 1a) or increase in HCl concentration (Figure 1b).

For octahedral complexes (centrosymmetric environment), the 1s−3d transition is an electric dipole forbidden transition. However, the small intensity of the pre-edge peak can be observed, attributed to an electric quadruple coupling.[12] For complexes in a non-centrosymmetric environment (e.g., tetrahedral coordination), the dipolar 1s−3d transition is allowed because of mixing of the 3d and 4p molecular orbitals, resulting in the increase in the pre-edge peak.[13] It was shown by Roe et al. that the intensity of the pre-edge peak decreases with an increase in the coordination number.[14] The intensities observed in 6- and 4-coordinated systems differ by a factor of 4,[14] which agrees well with our observations (see the inset of Figure 1a). The white line intensities agree as well with the results published by Testamale et al.[8] and with our interpretation that Fe ions have a tetrahedral coordination at small water or large HCl concentrations.

All spectra presented in Figure 1 show oscillations and intersect at some common points (7134, 7160, and 7190 eV in Figure 1a and 7142, 7167, and 7191 eV in Figure 1b). One may also say that all values of the absorption spectra lie between the values obtained for two "extreme" curves μ_1 and μ_2 for each series of samples; see the legends in Figure 1. This behavior indicates clearly that the spectra correspond to the mixture of two species with different weights. Indeed, let us consider two different, normalized spectra $\mu_1(E)$ and $\mu_2(E)$. They intersect at some points E_k, k = 1, 2, ..., which is equivalent to $\mu_1(E_k) = \mu_2(E_k)$. Any linear combination $\mu(E) = a\mu_1(E) + b\mu_2(E)$ with normalization condition $a + b = 1$ at points E_k has the value $\mu(E_k)$. It is easy to check that $\mu(E_k) = \mu_1(E_k) = \mu_2(E_k)$. This behavior is consistent with the results of analysis presented previously, where detailed analysis of measurements of extreme concentrations were presented.[6] The spectra were explained as resulting in two kinds of local Fe structures: tetrahedral and octahedral.

The energy of the K-edge is sensitive to the formal oxidation state of the absorbing atom; more precisely, the energy should increase with absorber effective charge.[1,10] On the other hand, Testamale et al. have shown that the absorption edge shift decreases when the number of ligands changes from 6 to 4 under constant oxidation state.[8] The same conclusion can be drawn from the investigation of Ti(IV) ions with 6, 5, and 4 ligand atoms.[15] In our XAS experiment, we observe a change in the local environment from octahedral to tetrahedral and no change in the position of absorption edge energy; see Figure 1. In this situation, we cannot exclude a possibility that iron in tetrahedral coordination is at the (III) oxidation state.

3.2. Mössbauer Measurements. To distinguish the oxidation state of iron ions in the different solutions, several Mössbauer spectra (see Figure 2) were recorded. A further

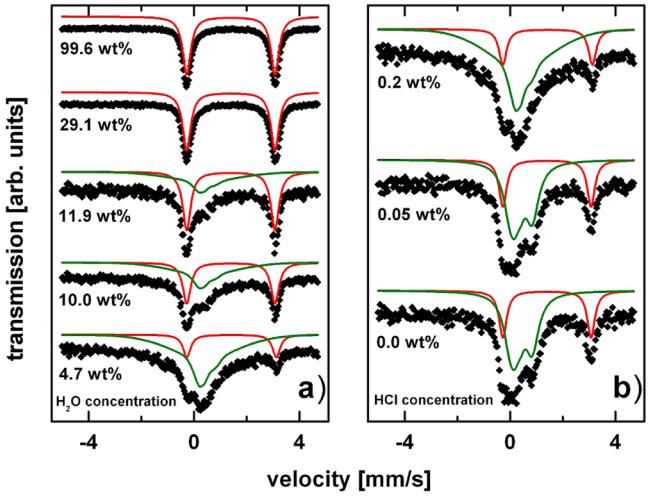

Figure 2. The Mössbauer spectra of frozen solutions as a function of (a) H_2O and (b) HCl concentration. Red and green curves correspond to Fe(II) and Fe(III) species, respectively. Spectra for 35.4 and 49.3 wt % H_2O have the same shape as the spectrum for 99.6 wt % H_2O, so they were omitted in the figure.

analysis will be made by comparison of the Mössbauer spectra of the frozen solutions prepared from $FeCl_2$ and $FeCl_3$, as shown in examples in Figure 3. The spectrum of divalent iron ion in water exhibits a simple ferrous high-spin doublet (Figure 3a) with isomer shift δ = 1.39(2) mm/s and quadrupole splitting Δ = 3.23(3) mm/s, consistent with parameters observed for iron ions in hexaaquo coordination.[16,17] The spectrum of $FeCl_3$ in frozen water solution (Figure 3d) shows poorly resolved hyperfine structure, typical for trivalent iron ion

dx.doi.org/10.1021/jp400556d | J. Phys. Chem. A 2013, 117, 2190−2194

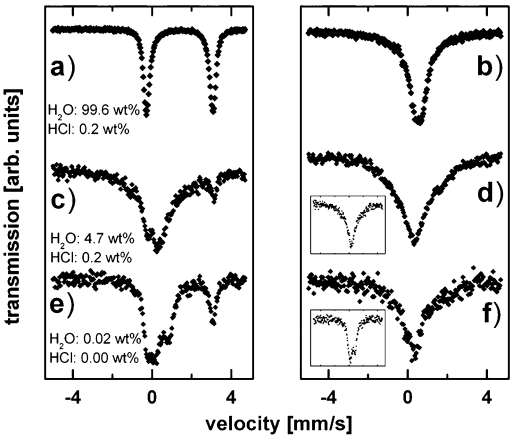

Figure 3. Mössbauer spectra for three end member solutions obtained from $FeCl_2$ (a, c, and e) and from $FeCl_3$ (b, d, and f). The insets show differences between spectra prepared from $FeCl_2$ and the ferrous high-spin doublet.

complexes. The average isomer shift is δ = 0.38(4) mm/s, in agreement with the reported value for $[FeCl_4]^-$.[18]

It is clear from Figure 3b that the Mössbauer spectra of acetone rich samples prepared from $FeCl_2$ can be composed of the spectrum of sample prepared from $FeCl_3$ and the ferrous high-spin doublet. By subtracting the ferrous high-spin doublet from $FeCl_2$ spectra, we get a shape almost the same as the shape of $FeCl_3$ spectra (see the inset in Figure 3d) and we are able to find the quantitative fraction of iron on the (III) oxidation state. Only in the case of $FeCl_2$ dissolved in almost pure acetone (Figure 3e) can we observe some additional doublet with isomer shift value characteristic for Fe(III).[18] Fractions of the ferrous components estimated from areas under the spectra are equal to 12.5% (Figure 3c) and 28.9% (Figure 3f) and are close to the values obtained from analysis of XAS spectra (10 and 20%, respectively). Contributions of Fe(II) and Fe(III) to the Mössbauer spectra of frozen solutions of $FeCl_2$ are shown in Figure 2 by solid lines and estimated fractions in Figure 5b.

Iron ions at the (II) oxidation state surrounded by Cl^- ligands were already observed in Mössbauer experiments with parameters δ = 1.01 mm/s and Δ = 0.61 mm/s for $[FeCl_4]^{2-}$ [18] and δ = 1.09 mm/s and Δ = 0.76 mm/s for $[FeCl_6]^{4-}$.[19] We do not observe components with so high isomer shifts and quadrupole splittings, other than the already discussed hexaaquo ferrous high-spin doublet. Therefore, formation of Fe(II) coordinated with Cl^- anions, if present, is at the level below the detection limit. Our Mössbauer results indicate clearly changes in the oxidation state of iron ions in acetone rich solutions.

3.3. Raman Measurements. The Raman spectra of $FeCl_2$ solutions are presented in Figure 4a. It is known that hydroxo complexes of iron ions exhibit the Fe−O bending mode around 195 cm^{-1} and Fe−O stretching modes in the range 442−523 cm^{-1}.[20] Unfortunately, those metal-to-ligand vibrations result in low intensity in the Raman spectrum.[21] Since the concentration of $Fe(H_2O)_6^{2+}$ in our samples is rather small, these modes were not detected. We were able to find only one Raman peak related to the presence of iron ions in the solutions, which corresponds to the strongest Fe−Cl stretching mode $\nu_1(A_1)$ for tetrahedral coordination, with Raman shift 332 cm^{-1}. The value agrees well with the reported 333 cm^{-1} for solids and solutions.[22] The intensity of this peak decreases with water concentration (e.g., increases with acetone content).

For quantitative characterization of the amount of iron atoms with tetrahedral coordination, also some other parts of Raman spectra were analyzed. We observe changes in peak intensities connected with acetone (395 cm^{-1} associated with the C−O out-of-plane bending mode, 1360 and 1432 cm^{-1} CH_3 deform modes, and 1710 cm^{-1} the C−O stretching mode)[23] and water (broad band at 1650 cm^{-1} associated with the O−H bending mode).[24] The observed 1710 cm^{-1} peak intensity is proportional to the acetone molar concentration, e.g., proportional to

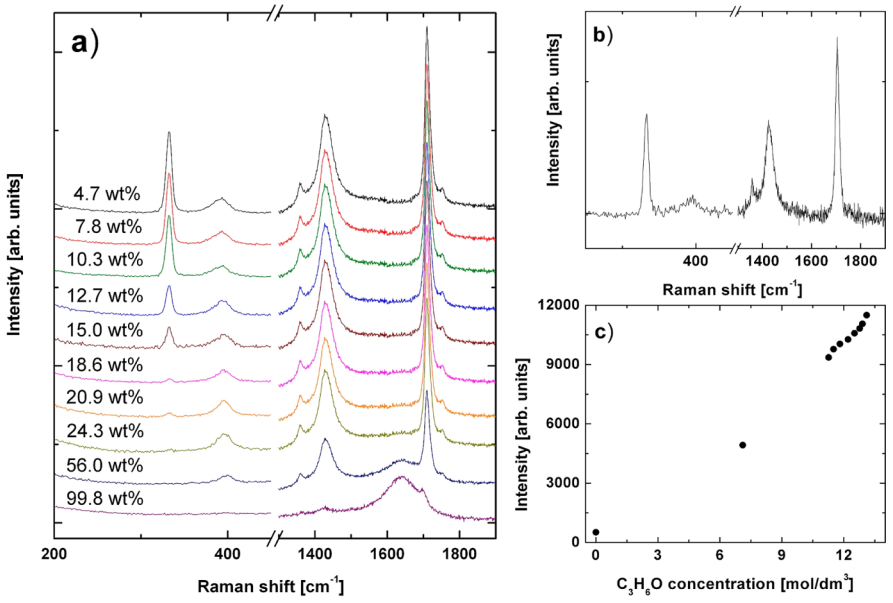

Figure 4. (a) Representative Raman spectra of the $FeCl_2$ solutions for different water concentrations. The region of Raman shift (450−1300 cm^{-1}) was omitted for clarity. (b) Reference spectrum of $FeCl_3$ in solution with 4.7 wt % H_2O. (c) Intensity of the Raman peak associated with the acetone CO stretching mode (1710 cm^{-1}) as a function of the acetone molar concentration.

dx.doi.org/10.1021/jp400556d | J. Phys. Chem. A 2013, 117, 2190−2194

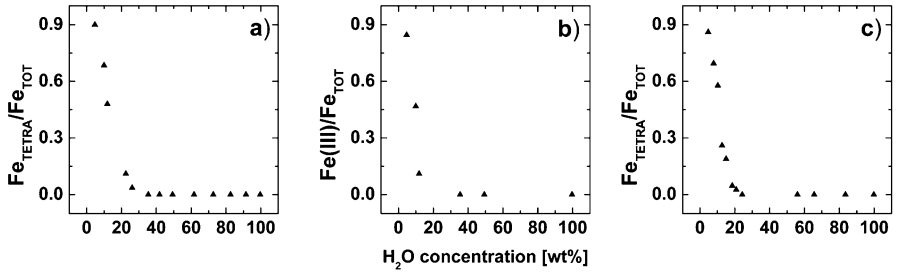

Figure 5. The results obtained from (a) XAS (fraction of iron ions in tetrahedral coordination), (b) Mössbauer (fraction of Fe(III) ions), and (c) Raman (fraction of $[FeCl_4]^-$) spectra.

the number of molecules interacting with the Raman beam (see Figure 4c).

Analogously to the result shown in Figure 4c, the intensity of the 332 cm^{-1} peak was used as a measure of the amount of iron in tetrahedral coordination. Part of the iron ions prepared from $FeCl_2$ in acetone rich solutions may have octahedral coordination, and this part, as already argued, is not visible in the Raman measurements. Therefore, the reference sample prepared with $FeCl_3$ was measured (Figure 4b). We have assumed that all Fe ions have a tetrahedral environment and the intensity of the 332 cm^{-1} peak was adopted as a measure of the amount of Fe ions coordinated by four Cl ions.

The analysis of results obtained for the sample with 4.7 H_2O wt % (one of the end-member solutions) shows that only 13.9% of iron ions exist in octahedral coordination. This result is consistent with XAS and Mössbauer experiments (20 and 12.5%, respectively).

Quantitative results obtained from XAS, Mössbauer, and Raman spectroscopies are presented in Figure 5.

All measurement techniques show consistent results of local structure of the iron ion in the $H_2O-C_3H_6O-HCl$ system. For a wide range of water concentration, iron ferrous ions are coordinated by six water molecules in octahedral symmetry. For acetone rich solutions (water concentration below 30 wt %), the change of symmetry from octa- to tetrahedral occurs. Change in ion symmetry is strongly correlated with the change in iron oxidation state. Mössbauer results indicate that the fraction of iron ions other than $Fe(H_2O)_6^{2+}$ is slightly smaller than the fraction of iron with tetrahedral coordination, determined from XAS and Raman experiments; see Figure 5. However, we can exclude formation of Fe(II) species with chloride ligands, such as $[FeCl_4]^{2-}$ or $[FeCl_6]^{4-}$. We do not observe the characteristic components for those complexes in Mössbauer spectra.

4. SUMMARY

The local structure and oxidation state of an iron ion in the $H_2O-C_3H_6O-HCl$ system was determined by Raman, X-ray absorption, and Mössbauer spectroscopies. The positions of Raman, pre-edge peaks, and hyperfine parameters are in good agreement with already published data. In aqueous solution, the first hydration shell of iron ions is octahedral $Fe(H_2O)_6^{2+}$, in agreement with what has been previously reported. In acetone rich solutions, part of the ferrous ions changed their oxidation state and formed the $[FeCl_4]^-$ tetrahedral complex. The Mössbauer spectra show unambiguously coexistence of $Fe(H_2O)_6^{2+}$ and Fe(III) species (Figure 2). The first-principle analysis of XAS spectra, performed under assumptions that octa- and tetrahedral local environments coexist,[6] agree well with the observed crossing of the XAS oscillations (Figure 1). Ions with octahedral environment were not observed in Raman experiments; however, combined measurements of samples prepared from $FeCl_2$ and $FeCl_3$ allow quantitative fractions of tetra- and octa-coordinated Fe ions to be obtained, in good agreement with the XAS and Mössbauer results.

AUTHOR INFORMATION

Corresponding Author

*E-mail: wojtek@alpha.uwb.edu.pl. Phone: +48 85/745 72 42. Fax: +48 85/745 72 23.

Notes

The authors declare no competing financial interest.

ACKNOWLEDGMENTS

We express our gratitude to Dr Hab. A. Wysmołek from University of Warsaw for discussions and preliminary Raman measurements. Portions of this research were carried out at the light source DORIS III at DESY, a member of the Helmholtz Association (HGF). We would like to thank E. Welter and D. A. Zając for assistance in using beamlines A1 and E4. The work was partially supported by EU funds under contract nos. I-20080184 EC and POPW.01.03.00-20-034/09-00, by the National Centre for Research and Development under the research project no. N R15 0117 10/NCBR, by the funds allocated for scientific research for the years 2008−2011 as a research project NN202172335, and by Podlaskie Scholarship Fund for the years 2012−2013.

REFERENCES

(1) Garcia, J.; Bianconi, A.; Benfatto, M.; Natoli, C. R. *J. Phys., Colloq.* **1986**, *47*, C8-49−C8-54.
(2) Benfatto, M.; Solera, J. A.; Chaboy, J.; Proietti, M. G.; Garcia, J. *Phys. Rev. B* **1997**, *56*, 2447−2452.
(3) D'Angelo, P.; Benfatto, M.; Della Longa, S.; Pavel, N. V. *Phys. Rev. B* **2002**, *66*, 064209.
(4) Szymański, K.; Olszewski, W. Polish Patent No. 207757, 2007.
(5) Olszewski, W.; Szymański, K.; Biernacka, M.; Sobiecki, R. *Mater. Sci.-Poland* **2008**, *26*, 122−129.
(6) Olszewski, W.; Szymański, K.; Zaleski, P.; Zając, D. A. *J. Phys. Chem. A* **2011**, *115*, 13420−13424.
(7) D'Angelo, P.; Benfatto, M. *J. Phys. Chem. A* **2004**, *108*, 4505−4514.
(8) Testamale, D.; Brugger, J.; Liu, W.; Etschmann, B.; Hazemann, J.-L. *Chem. Geol.* **2009**, *264*, 295−310.
(9) Lauher, J. W.; Ibers, J. A. *Inorg. Chem.* **1975**, *14*, 348−352.
(10) Benfatto, M.; Solera, J. A.; Ruiz, J. G.; Chaboy, J. *Chem. Phys.* **2002**, *282*, 441−450.
(11) Brand, R. A. *Normos-90 Mössbauer Fitting Program Package, User's Guide*; Wissenschaftliche Electronik GmbH: Starnberg, Germany, 1994.

(12) Schulman, R. G.; Yafet, Y.; Eisenberger, P.; Blumberg, W. E. *Proc. Natl. Acad. Sci. U.S.A.* **1976**, *73*, 1384−1388.
(13) Galoisy, L.; Calas, G.; Arrio, M. A. *Chem. Geol.* **2001**, *174*, 307−319.
(14) Roe, A. L.; Schneider, D. J.; Mayer, R. J.; Pyrz, J. W.; Widom, J.; Que, L., Jr. *J. Am. Chem. Soc.* **1984**, *106*, 1676−1681.
(15) Farges, F.; Brown, G. E., Jr.; Rehr, J. J. *Geochim. Cosmochim.* **1996**, *60*, 3023−3038.
(16) Vertes, A.; Nagy, D. L. *Mössbauer Spectroscopy of Frozen Solutions*; Akado Kiadó: Budapest, Hungary, 1990.
(17) Gütlich, P.; Bill, E.; Trautwein, A. X. *Mössbauer Spectroscopy and Transition Metal Chemistry*; Springer Verlag: Berlin, 1978.
(18) Feist, M.; Troyanov, S. I.; Mehner, H.; Witke, K.; Kemnitz, E. *Z. Anorg. Allg. Chem.* **1999**, *625*, 141−146 (in German).
(19) He, T.; Wang, J.; Chen, Z.; Wu, A.; Wu, G.; Yin, J.; Chu, H.; Xiong, Z.; Zhang, T.; Chen, P. *J. Mater. Chem.* **2012**, *22*, 7478−7483.
(20) Schouble, E. A.; Rossman, G. R.; Taylor, H. P., Jr. *Geochim. Cosmochim. Acta* **2001**, *65*, 2487−2497.
(21) Bonin, P. M. L.; Jędral, W.; Odziemkowski, M. S.; Gillham, R. W. *Corros. Sci.* **2000**, *42*, 1921−1939.
(22) Avery, J. S.; Burbridge, C. D.; Goodgame, D. M. L. *Spectrochim. Acta* **1968**, *24A*, 1721−1726.
(23) Cossee, P.; Schachtschneider, J. H. *J. Phys. Chem.* **1966**, *44*, 97−111.
(24) Carey, D. M.; Korenowski, G. M. *J. Chem. Phys.* **1998**, *108*, 2669−2675.